Title:

Heme's relevance genuine? Re-visiting the roles of TANGO2 homologs including HRG-9 and HRG-10 in *C. elegans*

Authors:

Sandkuhler, Sarah E.,[1] Youngs, Kayla S.,[2] Owlett, Laura,[2] Bandora, Monica B.,[3] Naaz, Aaliya,[4] Kim, Euri S.,[5] Wang, Lili,[6] Wojtovich, Andrew P.,[7] Gupta, Vandana A.,[5] Sacher, Michael,[4,8] Mackenzie, Samuel, J.[2]

Affiliations:

1 - Department of Pathology, University of Rochester Medical Center, Rochester, NY

2 - Department of Neurology, University of Rochester Medical Center, Rochester, NY

3 - Morgan State University, Baltimore, MD

4 - Department of Biology, McGill University, Montreal, Canada

5 - Department of Medicine, Brigham and Women's Hospital Harvard Medical School, Boston, MA

6 - Department of Pharmacology, Vanderbilt University, Nashville, TN

7 - Department of Anesthesiology and Perioperative Medicine, University of Rochester Medical Center, Rochester, NY

8 - Department of Anatomy and Cell Biology, Concordia, Montreal, Canada

Corresponding Author:

Samuel J. Mackenzie

University of Rochester Medical Center

Room 1-9644 KMRB

601 Elmwood Ave

Rochester, NY 14642

Samuel_mackenzie@urmc.rochester.edu

585-276-6503

Abstract:

Mutations in the *TANGO2* gene cause severe illness in humans, including life-threatening metabolic crises. However, the function of TANGO2 protein remains unknown. Using *Caenorhabditis elegans* and other models, it has recently been proposed that TANGO2 transports heme within and between cells, from areas with high heme concentrations to those with lower concentrations. Here, we demonstrate that heme-related observations in nematodes may be better explained by a previously unreported metabolic phenotype in these worms, characterized by reduced feeding, decreased lifespan and brood sizes, and poor motility. We also show that several genes not implicated in heme transport are upregulated in the low heme state and conversely demonstrate that *hrg-9* in particular is highly responsive to oxidative stress, independent of heme status. Collectively, these data implicate bioenergetic failure and oxidative stress as key factors in the pathophysiology of TANGO2 deficiency, in alignment with observations from human patients. Our group performed several experiments in yeast and zebrafish deficient in TANGO2 homologs and was unable to replicate prior findings from these models. Overall, we believe there is insufficient evidence to support heme transport as the primary function for TANGO2.

Introduction:

Transport and Golgi Organization 2 (TANGO2) Deficiency Disorder (TDD) is associated with a severe progressive neurodegenerative disease in children and young adults, frequently accompanied by recurrent, life-threatening metabolic crises.[1-4] While TANGO2 is conserved in species across all three kingdoms of life, its cellular function has not been fully elucidated. Initially identified in a screen of *Drosophila* genes associated with ER-Golgi fusion,[5] TANGO2 has since been shown to localize to both the cytoplasm and the mitochondria.[6] Mutations in TANGO2 have been associated with altered mitochondrial respiration and morphology,[7] disregulated lipid homeostasis[8,9] and defects in fatty acid oxidation[7] in multiple models. Treatment with supplemental pantothenic acid, the precursor of coenzyme A, has been shown to improve lipid profile abnormalities in cells,[9] rescue phenotypic defects in a *Drosophila* TDD model,[10] and potentially reduce metabolic crises in patients,[11] suggesting a central role for coenzyme A (CoA) and lipid homeostasis in the pathophysiology of TDD.

A recent study by Sun et al. reported that two *Caenorhabditis elegans* homologs of TANGO2, HRG-9 and HRG-10 (Heme-Responsive Gene), play a critical role in heme export from intestinal cells and lysosome-related organelles and that TANGO2 exhibits a similar function in mobilizing heme from mitochondria in other eukaryotic organisms including yeast.[12] Two subsequent studies also implicated TANGO2 in heme transport albeit via discordant intracellular mechanisms.[13,14] The notion that defective heme transport underlies the pathophysiology of TANGO2 deficiency marks a sizeable shift from the emerging scientific consensus related to the role of TANGO2 in CoA and lipid handling. We hypothesize that these apparent defects in heme transport may be downstream features of aberrant cellular metabolism and may not be central to the pathophysiology of TDD.

Results:

<u>*C. elegans* lacking TANGO2 homologs (double knockout; DKO) demonstrate modest survival benefit upon toxic heme analog exposure</u>

We first sought to validate results from prior experiments using heme analogs in worms lacking both HRG-9 and HRG-10 (double knockout; DKO). In previous studies, DKO worms exposed to 1 µM concentration of the toxic heme analog gallium protoporphyrin IX (GaPP) showed a significant survival benefit contrasted with the nearly uniform lethality in wild type (Bristol N2) worms.[12] We exposed gravid DKO and N2 nematodes to GaPP at varying concentrations, removing P_0 worms at 24 hours, and counting alive and dead F_1 progeny at 72 hours. While we required relatively higher concentrations of GaPP to achieve lethality, all strains exhibited a clear dose-dependent reduction in survival (Fig. 1A). A statistically significant group effect was seen at the 2 µM concentration with a relative survival benefit in DKO worms, though the difference between DKO and N2 worms was more modest than previously reported.

DKO *C. elegans* demonstrate increased lawn avoidance and reduced pharyngeal pumping

In maintaining the DKO strain under basal conditions (i.e., no GaPP exposure), we incidentally observed relatively intact *E. coli* lawns on plates housing DKO worms compared to N2 plates. On closer examination, DKO worms demonstrated several previously undescribed phenotypic features including lawn avoidance, a greater propensity for crawling off plates, reduced pharyngeal pumping, and decreased survival (Fig. 2A, B, F). Based on these observations, we hypothesized that the GaPP survival difference in our initial experiment might have been driven, at least in part, by reduced GaPP consumption. We therefore also examined the effect of GaPP exposure on worms missing a pharyngeal acetylcholine receptor subunit (*eat-2*(*ad465*)). The *eat-2* strain exhibits reduced pharyngeal pumping and has been used extensively as a model of dietary restriction.[15,16] Of the three strains tested, survival was highest in *eat-2* mutants (Fig.1A) despite the fact that these worms have no known defects in heme metabolism or transport.

DKO *C. elegans* demonstrate reduced ZnMP fluorescence

Sun et al. previously reported that DKO nematodes accumulate the fluorescent heme analog zinc mesoporphyrin IX (ZnMP) in intestinal cells after exposure in low-heme (4 µM) liquid media. To determine whether this effect persisted under basal conditions on standard OP50 *E.*

coli NGM plates, we exposed L4 nematodes to 40 μM ZnMP and imaged them after 16 hours. Contrary to prior results, we found that DKO worms demonstrated significantly reduced intestinal ZnMP fluorescence compared to N2 (Fig.1B). To test whether stress-induced gut granule autofluorescence secondary to heme deficiency may have contributed to the higher fluorescent intensities previously reported, we repeated this experiment under starved conditions and showed a marginal, albeit nonsignificant, increase in intestinal fluorescence. Given that this increase was comparable between DKO and N2 worms, we believe that autofluorescence is unlikely to account for their reported group difference.

DKO *C. elegans* demonstrate multiple features suggestive of bioenergetic dysfunction

In assessing brood survival in the GaPP assay, we also observed significantly smaller starting broods for DKO nematodes, a finding that persisted in the absence of GaPP (Fig.2C). As oogenesis and egg-laying require a high energetic expenditure for gravid *C. elegans*, reduced brood size is a known feature of several metabolically impaired nematode strains.[17,18] We also incidentally noticed reduced movement on the plate from DKO worms and decided to further characterize the worms' capacity for movement by subjecting them to a swim exhaustion assay. Nematodes were placed in isotonic M9 buffer and scored on their swimming ability at 4 minute intervals. While *C. elegans* are typically able to swim continuously for up to 90 minutes in M9 media,[19] we observed that the DKO worms quickly became exhausted and could not maintain normal swimming shortly after being placed in media (Fig. 2D). We further quantified the rate of thrashing in M9 media during the first 4 minute interval and found that DKO worms thrashed 61% slower compared to N2s (Fig. 2E). Together, these results are suggestive of a potential bioenergetic defect arising from TANGO2 homolog deficiency.

Oxidative stress is a transcriptional driver of TANGO2 homolog expression

Given previous observations implicating oxidative stress as a feature of TDD,[7] we next sought to determine what other genes were enriched under low heme conditions. We reanalyzed the RNA-seq dataset generated by Sun et al., employing the Empirical Analysis of Gene Expression in R (edgeR) package on raw counts to accurately perform between-group

comparisons across low (2 µM), optimal (20 µM), and high (400 µM) heme conditions. We extracted the top 500 enriched genes and plotted those that showed significantly increased expression in the low heme state, based on computational clustering (N=134; Fig. 3A). Several genes with no known heme-related functions demonstrated stronger relative expression and higher likelihood ratios of conditional effect than did *hrg-9*. Furthermore, gene ontology analysis of genes with similar enrichment to *hrg-9* revealed a wide spectrum of biological processes and cellular roles, including but not limited to collagen deposition, cellular detoxification, and lipid binding (Fig. 3B). To test what alternate forms of cell stress might induce *hrg-9* and *hrg-10* expression, we exposed N2 nematodes to heat (34°C), starvation (24 hours without OP50), and paraquat, a potent generator of reactive oxygen species (25 mM), before performing RT-qPCR. We observed a 12-fold enrichment of *hrg-9* after paraquat exposure, suggesting that its expression may be linked to cellular stress more broadly and is not uniquely driven by heme levels (Fig. 3C).

Yeast deficient in TANGO2 homolog YGR127w exhibit normal growth

As Sun et al. also examined the function of TANGO2 homologs in yeast (YGR127w) and zebrafish (tango2), we sought to validate their findings in these models. Sun et al. reported a severe temperature sensitive growth defect and impaired heme distribution in the *ygr127w* yeast knockout. We also observed a growth defect in their strain. However, two separate strains on different backgrounds (BY4741 and BY4742) and a third strain generated by our lab (W303-1a) showed normal growth (Fig. 4A). The growth defect in their strain was also not rescued with YGR127w complementation. As the background used by Sun et al. is known to be prone to mitochondrial genome instability,[20] we hypothesize that their line may harbor a secondary mutation.

Myofiber defects in tango2-deficient zebrafish

In zebrafish, Sun et al. reported no discernable phenotype in *tango2*$^{-/-}$ fish bred from heterozygous parents but observed severe skeletal muscle damage in *tango2*$^{-/-}$ larvae from *tango2*$^{-/-}$ parents. In a recent study, we showed increased lethality and reduced phospholipid

and triglyceride levels in *tango2*$^{-/-}$ fish obtained from heterozygous parents.[21] *tango2*$^{-/-}$ larvae from two different alleles (tango2^{bwh210} and tango2^{bwh211}) exhibited defects in myofiber organization irrespective of heterozygous or homozygous parents (Fig. 4B) but lacked the striking muscle damage reported by Sun et al.

Discussion:

In this study, we attempted to replicate prior observations related to defective heme transport in a *C. elegans* model lacking TANGO2 homologs but were ultimately unable to do so. Additionally, we noted several previously unreported phenotypic characteristics that suggest a broader bioenergetic defect in these worms, reminiscent of what has been observed in patients with TDD. In our experiments with yeast and zebrafish, we were also unable to replicate central findings pertaining to growth and muscle fiber integrity, respectively.

Our data and collective clinical experience with TDD do not support the notion that TANGO2 primarily functions as a heme chaperone. Laboratory abnormalities in TDD include abnormal acylcarnitine profiles, hyperammonemia, and elevated creatinine kinase levels during metabolic crises,[3,11] while abnormalities associated with defective heme transport (e.g., erythrocyte membrane defects, low hemoglobin levels) have not been linked with the disease. Strikingly, retrospective data suggest that patients with TDD receiving B-vitamin supplementation inclusive of pantothenic acid, a precursor of coenzyme A, do not experience metabolic crises[11] and show substantial improvement in other domains as well. Pantothenic acid supplementation also yielded full phenotypic rescue in a *Drosophila* model of the disease.[10] It is difficult to reconcile how this treatment would be beneficial in a disease characterized by dysregulated heme trafficking.

Heme is a hydrophobic molecule, thus it is plausible that if TANGO2 and its homologs are involved in lipid handling, these proteins may also weakly bind heme.[13] Han et al. demonstrated that a bacterial heme homolog, HtpA, directly binds heme and is necessary for cytochrome *c* function.[13] We would note, however, that TANGO2 was not among the 378 heme-

binding proteins identified on a recent proteomic screen of three separate cell lines.[22] Jayaram et al. proposed that TANGO2 functions instead by interacting with FLVCR1b to release mitochondrial heme without directly binding to heme itself, though this interaction was observed only after heme synthesis was potentiated via d-ALA and iron supplementation, raising questions about the role of TANGO2 under basal conditions.[14] Furthermore, in this study, GAPDH was identified as the exclusive binding partner of heme upon export through FLVCR1b. How GADPH, a protein important for multiple cellular functions, including glycolysis, is affected in TDD remains unknown.

Although we believe there is currently insufficient evidence to suggest that TANGO2 is primarily involved in heme transport, more work is clearly needed to elucidate the cellular function of this important and highly conserved protein. This knowledge will be critical as we work to develop effective treatments for patients with TDD.

Materials and methods:

Worm strains and maintenance: Worm strains used include Bristol N2 (obtained from Caenorhabditis Genetics Center (CGC) at the University of Minnesota), DKO (CCH303 (hrg-9(cck301)V; hrg-10(cck302)V) obtained from C. Chen, and eat-2(ad465), obtained from the Samuelson lab at the University of Rochester. All worms were maintained at 20º C on standard nematode growth medium (NGM) plates with OP50 *E. coli.* All *C. elegans* assays were performed and scored by blinded observers.

GaPP survival assay: Adult worms were placed on standard OP50 NGM plates treated with 1, 2, 5, or 10 µM gallium protoporphyrin IX (Santa Cruz) and permitted to lay eggs for 24 hours then removed. Offspring were assessed 72 hours later for survival and were scored as dead if they did not respond to prodding with a platinum wire worm pick.

Pharyngeal pumping: L4 worms were observed and video recorded for 60 second intervals. The number of pharyngeal pumps per minute was manually counted.

Lawn avoidance: L4 worms were placed in the center of OP50 *E. coli* lawns on standard NGM plates and incubated at 20º C for 24 hours. Plates were examined 24 hours later and the numbers of worms remaining on the lawn or on unseeded agar were counted. Worms found on the sides of the dish or otherwise absent from NGM surface were scored as off the plate.

Brood size: For 24-hour brood assessments, young adult worms were placed on plates and allowed to lay eggs for 24 hours before being removed. Viable offspring were counted 48 hours later. For total brood assessments, L4 worms were placed on plates and moved to fresh plates every 24 hours for 5 days to ensure all eggs were accounted for. Viable offspring from eggs laid on each plate were counted 48 hours later and summed.

ZnMP fluorescence: L4 worms were placed on plates treated with 40 µM Zinc mesoporphyrin IX (Santa Cruz) for 16 hours before being washed in M9 buffer, anesthetized in sodium azide, and mounted on slides with 2% agarose pads for imaging. Worms in the starved condition were placed on unseeded plates for 16 hours before preparation and mounting as above. Worms were imaged on an EVOS 5000 microscope with consistent acquisition parameters. Fluorescent intensity within the proximal worm intestine was measured in ImageJ.

RNA-seq cluster and gene ontology analysis: The RNA sequencing (RNA-seq) dataset generated by Sun et al. was analyzed with Empirical Analysis of Gene Expression in R (edgeR) and the top 500 genes were extracted. Computational cluster analysis was done in RStudio. Gene ontology analysis was performed on significantly enriched genes using WormCat.[23] Source code is available in supplemental materials.

Stress conditions and RT-qPCR: N2 worms were subjected to the following stress conditions prior to RNA extraction: 1) fasting: worms were deprived of OP50 E. coli for 24 hours; 2) heat: worms were incubated for 4 hours at 34º C; 3) paraquat: worms were placed on standard NGM/OP50 plates treated with 25 mM paraquat (methyl viologen; Sigma Aldrich) for 24 hours. Whole worm RNA was extracted with TriZol (Invitrogen) and treated with RNeasy Mini Kit (Qiagen). cDNA generation was performed with Maxima First Strand cDNA synthesis kit (Thermo Fisher). qPCR was performed in triplicate using iTaq Universal SYBR (Invitrogen) with a CFX Duet Realtime qPCR machine (BioRad). Gene expression was normalized to worm *act* and analyzed using the ΔΔCq method. Primers used were as follows:

hrg-9: GGACCCGCTGCCATACACTAATC and GACAATTCAAATCTGGCATCGTG

hrg-10: AGGCTTCCCGGAGCACATTTAC and CAGGCTCCATGCGTCTATCCAG

act: CAACACTGTTCTTTCCGGAG and CTTGATCTTCATGGTTGATGGG

Yeast strain construction: *YGR127w* was knocked out by homologous recombination. A strain (BY4741) harboring a *ygr127w*D was used as a template and the knockout cassette was amplified by PCR using the following primers that anneal upstream and downstream of the locus: TTGGCATCTGCCTAGCTTTCG and AGCGTCTACTGTGGTTACTG

The PCR amplicon was then transformed into W303-1a cells and transformants were selected on YPD plates containing 200mg/ml G418. Integration at the correct locus was confirmed by PCR using the same primers, as above. To complement the *ygr127w*D in the Sun et al. strain, wild type *YGR127w* was amplified with 400 base pairs on either side of the gene and cloned into a *HIS3*-containing plasmid (pRS413). Transformants were selected on synthetic complete (SC) medium lacking histidine.

Yeast growth curves: Cells were grown to stationary phase at 25°C in either SC or SC-histidine medium. Cultures in the same medium were inoculated at an OD600 of ~0.01 in a 100ml volume in a 96-well plate. The OD600 was read every 15 minutes on a Sunrise Tecan microplate reader.

Zebrafish: All procedures involving zebrafish were approved by the Brigham and Women's Hospital Animal Care and Use Committee. Fish were bred and maintained using standard methods as described.[24] tango2bwh210 and tango2bwh211 zebrafish lines were created in our laboratory by the CRISPR-Cas9 approach as described previously.[21] The tango2bwg210 allele has an insertion of seven bases (c.226_227ins7; p.Tyr76Leufs*25) and tango2bwg211 has a 26 base insertions in exon2 (c.226_227ins26; p.Tyr76Leufs*207) resulting in frameshift mutations and loss of protein function. Whole mount phalloidin staining and microscopy was performed as described previously.[25]

Statistics and Reproducibility: All statistical analyses were performed in GraphPad Prism 9. Data presented are mean ± S.E.M. One-way analysis of variance (ANOVA) followed by Bonferroni's multiple comparisons was used to determine statistical significance ($p < 0.05$). Sample sizes were not pre-determined.

Contributions:

SJM, SES, KSY, APW, and LW designed the *C. elegans* experiments. SES, KSY, and MBB performed the *C. elegans* experiments and analyzed the data. LDO performed the RNA-seq analysis. MS designed the yeast experiments. PA performed the yeast experiments and analyzed the data. VAG and ESK designed the zebrafish experiments, and EK performed these

experiments. VAG and ESK analyzed the zebrafish data. SJM and SES wrote the initial draft of the manuscript. All authors reviewed the manuscript and contributed to its final version.

Acknowledgements:

The authors would like to thank Dr. Keith Nehrke and Dr. Paul Brookes for their guidance and manuscript review, the Chen lab for providing the *hrg-9*/*hrg-10* knockout nematode strain, and the Samuelson lab for supplying the *eat-2* nematode strain. SES is a trainee in the Medical Scientist Training Program funded by NIH T32 GM007256. SJM is supported by National Institutes of Health (NIH) National Institute of Neurological Disorders and Stroke Grant #2K12NS098482-06. This work was funded in part by grants from the TANGO2 Research Foundation to VAG, MS, and to SJM and LW.

Competing Interests:

The authors declare the following competing interests:

The following authors have unpaid roles at the TANGO2 Research Foundation:

SES, Early Diagnostic and Detection Committee Member

VAG, Scientific Advisor Board Member

MS, Executive Board Member

SJM, Research Committee Member and Scientific Advisory Board Chair

Data Availability Statement:

All raw data from worm behavior, yeast, zebrafish, and RNA-seq studies are available as a supplement to this paper.

References:

1 Kremer, L. S. *et al.* Bi-allelic Truncating Mutations in TANGO2 Cause Infancy-Onset Recurrent Metabolic Crises with Encephalocardiomyopathy. *Am J Hum Genet* **98**, 358-362 (2016). https://doi.org:10.1016/j.ajhg.2015.12.009

2 Lalani, S. R. *et al.* Recurrent Muscle Weakness with Rhabdomyolysis, Metabolic Crises, and Cardiac Arrhythmia Due to Bi-allelic TANGO2 Mutations. *Am J Hum Genet* **98**, 347-357 (2016). https://doi.org:10.1016/j.ajhg.2015.12.008

3 Powell, A. R., Ames, E. G., Knierbein, E. N., Hannibal, M. C. & Mackenzie, S. J. Symptom Prevalence and Genotype-Phenotype Correlations in Patients With TANGO2-Related Metabolic Encephalopathy and Arrhythmias (TRMEA). *Pediatr Neurol* **119**, 34-39 (2021). https://doi.org:10.1016/j.pediatrneurol.2021.02.011

4 Jennions, E. *et al.* TANGO2 deficiency as a cause of neurodevelopmental delay with indirect effects on mitochondrial energy metabolism. *J Inherit Metab Dis* **42**, 898-908 (2019). https://doi.org:10.1002/jimd.12149

5 Bard, F. *et al.* Functional genomics reveals genes involved in protein secretion and Golgi organization. *Nature* **439**, 604-607 (2006). https://doi.org:10.1038/nature04377

6 Milev, M. P. *et al.* The phenotype associated with variants in TANGO2 may be explained by a dual role of the protein in ER-to-Golgi transport and at the mitochondria. *J Inherit Metab Dis* **44**, 426-437 (2021). https://doi.org:10.1002/jimd.12312

7 Heiman, P. *et al.* Mitochondrial dysfunction associated with TANGO2 deficiency. *Sci Rep* **12**, 3045 (2022). https://doi.org:10.1038/s41598-022-07076-9

8 Lujan, A. L. *et al.* Defects in lipid homeostasis reflect the function of TANGO2 in phospholipid and neutral lipid metabolism. *Elife* **12** (2023). https://doi.org:10.7554/eLife.85345

9 Mehranfar, M. *et al.* Lipidomic analysis of human TANGO2-deficient cells suggests a lipid imbalance as a cause of TANGO2 deficiency disease. *Biochem Biophys Res Commun* **717**, 150047 (2024). https://doi.org:10.1016/j.bbrc.2024.150047

10 Asadi, P., Milev, M. P., Saint-Dic, D., Gamberi, C. & Sacher, M. Vitamin B5, a coenzyme A precursor, rescues TANGO2 deficiency disease-associated defects in Drosophila and human cells. *J Inherit Metab Dis* (2022). https://doi.org:10.1002/jimd.12579

11 Miyake, C. Y. *et al.* Natural History of TANGO2 Deficiency Disorder: Baseline Assessment of 73 Patients. *Genet Med* (2022). https://doi.org:10.1016/j.gim.2022.11.020

12 Sun, F. *et al.* HRG-9 homologues regulate haem trafficking from haem-enriched compartments. *Nature* **610**, 768-774 (2022). https://doi.org:10.1038/s41586-022-05347-z

13 Han, S., Guo, K., Wang, W., Tao, Y. J. & Gao, H. Bacterial TANGO2 homologs are heme-trafficking proteins that facilitate biosynthesis of cytochromes c. *mBio* **14**, e0132023 (2023). https://doi.org:10.1128/mbio.01320-23

14 Jayaram, D. T. *et al.* Heme allocation in eukaryotic cells relies on mitochondrial heme export through FLVCR1b to cytosolic GAPDH. *Res Sq* (2024). https://doi.org:10.21203/rs.3.rs-4314324/v1

15 Lakowski, B. & Hekimi, S. The genetics of caloric restriction in Caenorhabditis elegans. *Proc Natl Acad Sci U S A* **95**, 13091-13096 (1998). https://doi.org:10.1073/pnas.95.22.13091

16 Greer, E. L. & Brunet, A. Different dietary restriction regimens extend lifespan by both independent and overlapping genetic pathways in C. elegans. *Aging Cell* **8**, 113-127 (2009). https://doi.org:10.1111/j.1474-9726.2009.00459.x

17 Van Raamsdonk, J. M. *et al.* Decreased energy metabolism extends life span in Caenorhabditis elegans without reducing oxidative damage. *Genetics* **185**, 559-571 (2010). https://doi.org:10.1534/genetics.110.115378

18 Byrne, J. J. *et al.* Disruption of mitochondrial dynamics affects behaviour and lifespan in Caenorhabditis elegans. *Cell Mol Life Sci* **76**, 1967-1985 (2019). https://doi.org:10.1007/s00018-019-03024-5

19 Ghosh, R. & Emmons, S. W. Episodic swimming behavior in the nematode C. elegans. *J Exp Biol* **211**, 3703-3711 (2008). https://doi.org:10.1242/jeb.023606

20 Dimitrov, L. N., Brem, R. B., Kruglyak, L. & Gottschling, D. E. Polymorphisms in multiple genes contribute to the spontaneous mitochondrial genome instability of Saccharomyces cerevisiae S288C strains. *Genetics* **183**, 365-383 (2009). https://doi.org:10.1534/genetics.109.104497

21 Kim, E. S. *et al.* Intrinsic and extrinsic regulation of rhabdomyolysis susceptibility by Tango2. *Dis Model Mech* **16** (2023). https://doi.org:10.1242/dmm.050092

22 Homan, R. A., Jadhav, A. M., Conway, L. P. & Parker, C. G. A Chemical Proteomic Map of Heme-Protein Interactions. *J Am Chem Soc* **144**, 15013-15019 (2022). https://doi.org:10.1021/jacs.2c06104

23 Holdorf, A. D. *et al.* WormCat: An Online Tool for Annotation and Visualization of Caenorhabditis elegans Genome-Scale Data. *Genetics* **214**, 279-294 (2020). https://doi.org:10.1534/genetics.119.302919

24 Westerfield, M. *The Zebrafish Book: A Guide for the Laboratory Use of Zebrafish (Danio Rerio)*. (Institute of Neuroscience. University of Oregon, 2000).

25 Casey, J. G. *et al.* NRAP reduction rescues sarcomere defects in nebulin-related nemaline myopathy. *Hum Mol Genet* **32**, 1711-1721 (2023). https://doi.org:10.1093/hmg/ddad011

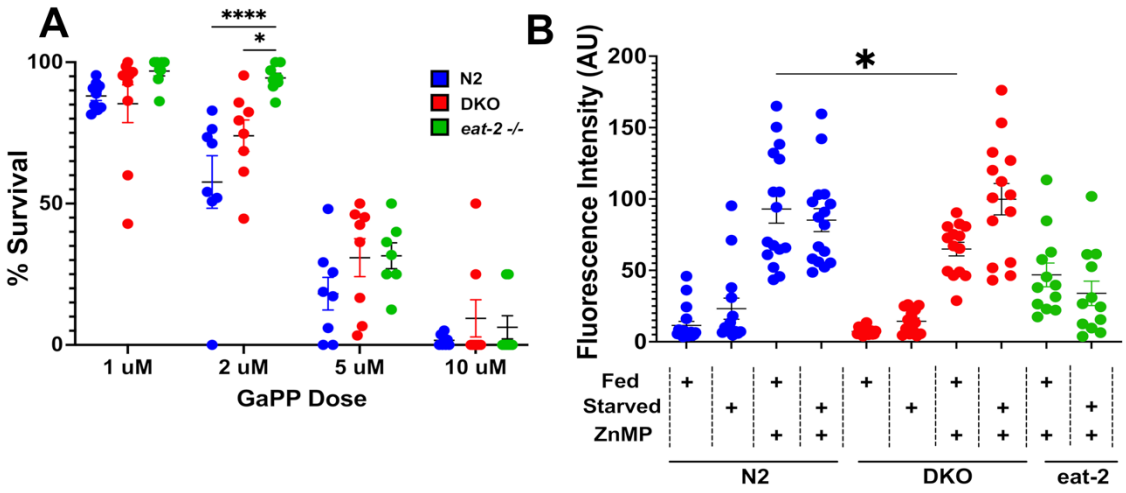

Figure 1: Reduced uptake of toxic and fluorescent heme analogs may explain marginal differences observed between wildtype *C. elegans* and nematodes lacking HRG-9 and HRG-10 (double knockout; DKO).

A) Survival of N2, DKO, or *eat-2* knockout worms exposed to 1, 2, 5, or 10 µM GaPP for 72 hours. N=3 independent experiments. * $p<0.05$, **** $p<0.0001$ **B)** Quantification of fluorescent staining in N2, DKO, and *eat-2* worms under fed and starved conditions with or without 40 µM ZnMP treatment. A.U. arbitrary units, N=15 worms analyzed over 3 independent experiments. * $p<0.05$.

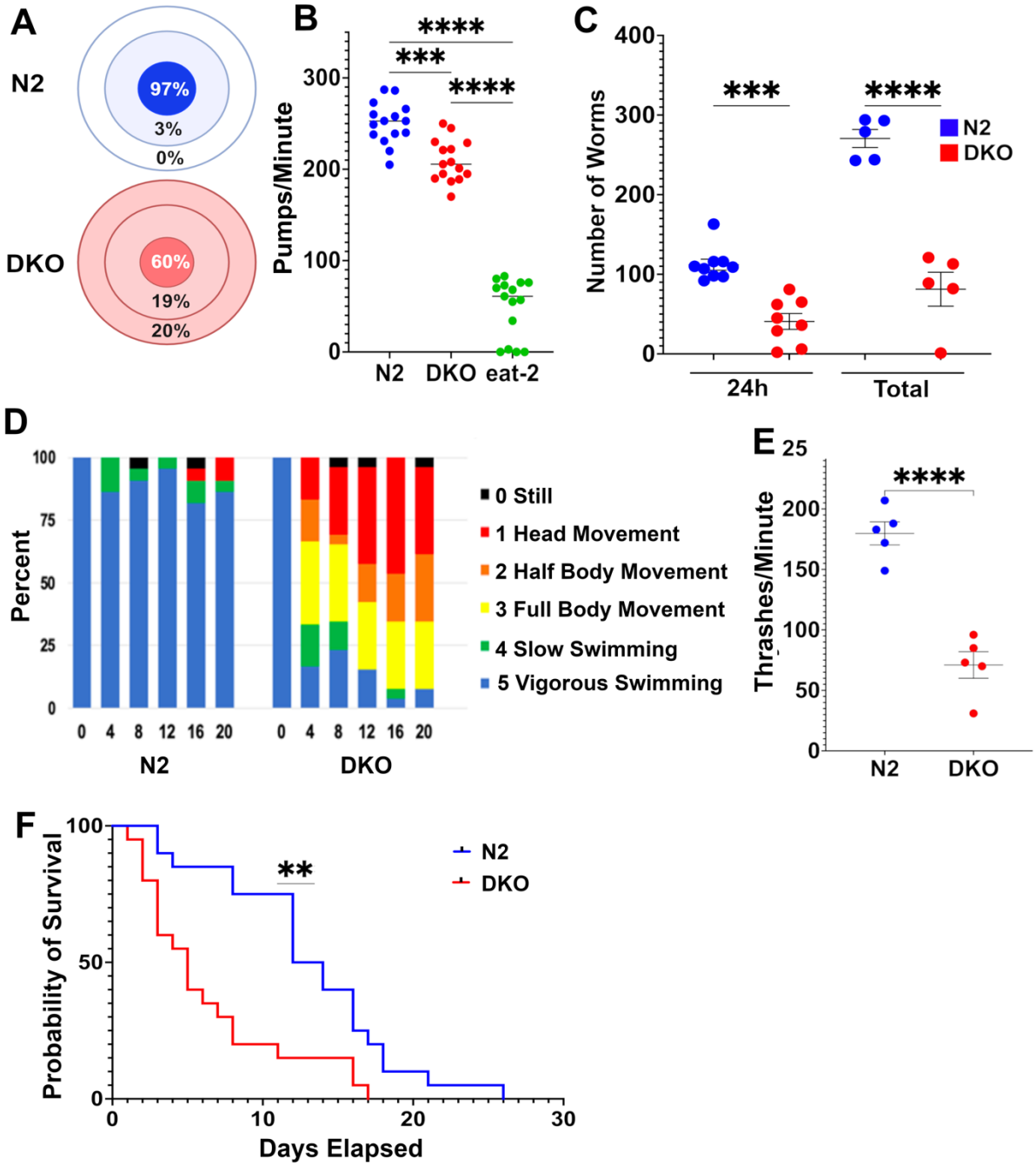

Figure 2: DKO nematodes demonstrate lawn avoidance and reduced pharyngeal pumping, brood sizes, motility, and survival.

A) Proportion of N2 or DKO worms present on OP50 lawn (innermost ring), off OP50 lawn (middle ring), or missing or dead from NGM plate (outer ring). N=180 worms over 3 independent experiments **B)** Number of of pharyngeal pumps in a one-minute period in N2, DKO, and *eat-2* knockout worms. N=15 worms over 3 independent experiments **C)** Number of viable offspring laid by single adult N2 or DKO worms either after 24 hours of egg lay or across total egg-laying period (5 days). N=8 broods for 24-hour counts, N=5 broods for total brood size counts. **D)** Swimming behavior of N2 and DKO worms over a 20 minute interval**.** Worms were observed at 4 minute intervals and scored from 0-5 on swimming intensity. Bars represent the proportion of worms at each score. **E)** Quantification of thrashes after 4 minutes in M9 buffer. **F)** Longevity of N2 and DKO C. elegans observed from L4 larval stage. N=30 worms over 3 independent experiments. (** $p<0.01$, *** $p<0.001$, **** $p<0.0001$).

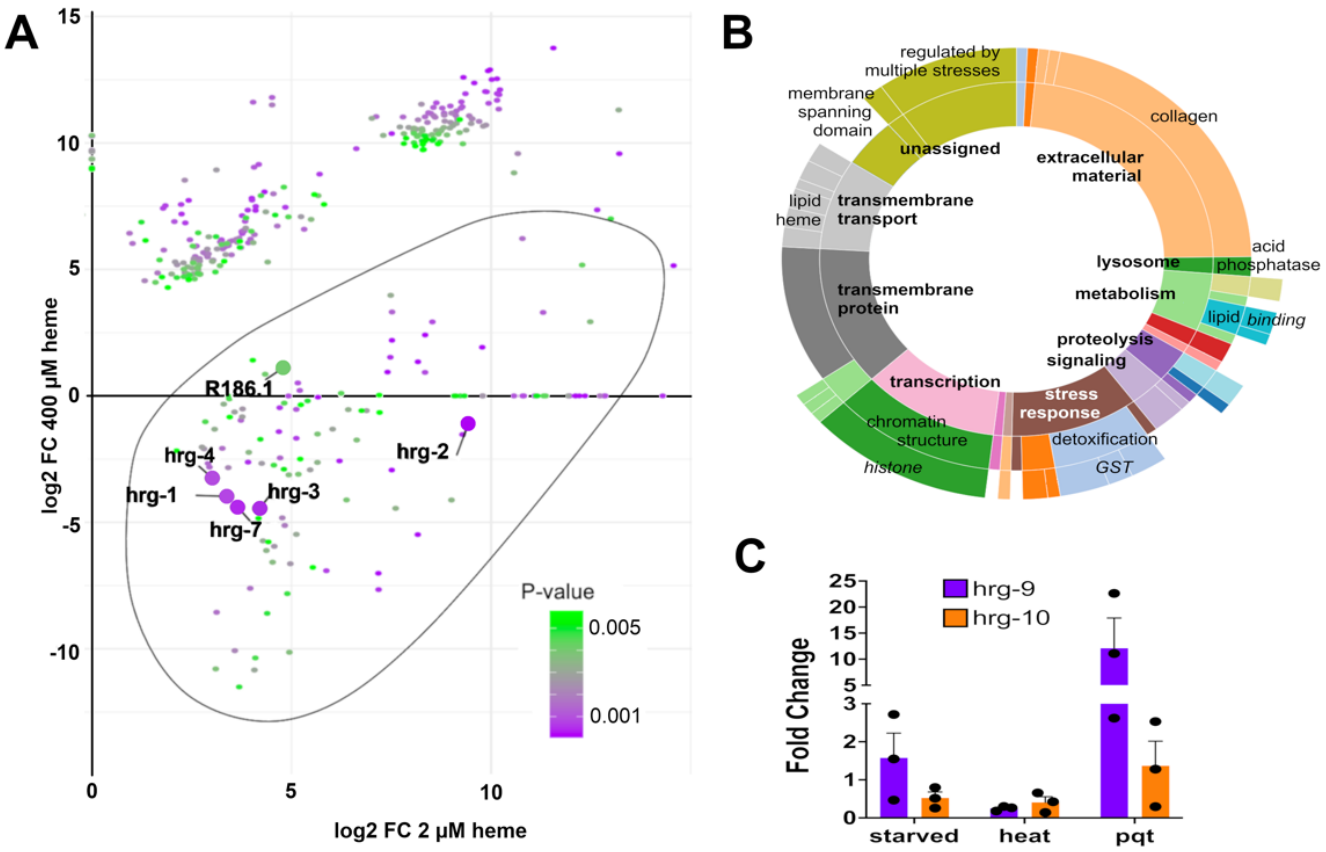

Figure 3: RNA-seq and qPCR analysis show that *hrg-9* and *hrg-10* are not uniquely heme responsive and may be linked to oxidative stress.

A) Analysis of top 500 genes with differential expression under low heme (2 µM) and high heme (400 µM) conditions. Outline represents 134 relevant genes identified by cluster analysis. **B)** Gene ontology analysis identified a variety of biological roles for genes within this cluster **C)** RT-qPCR of *hrg-9* and *hrg-10* under non-heme stress conditions: 24-hour starvation, 4-hour exposure to 34º C heat, and 25 mM paraquat. N=3 independent experiments.

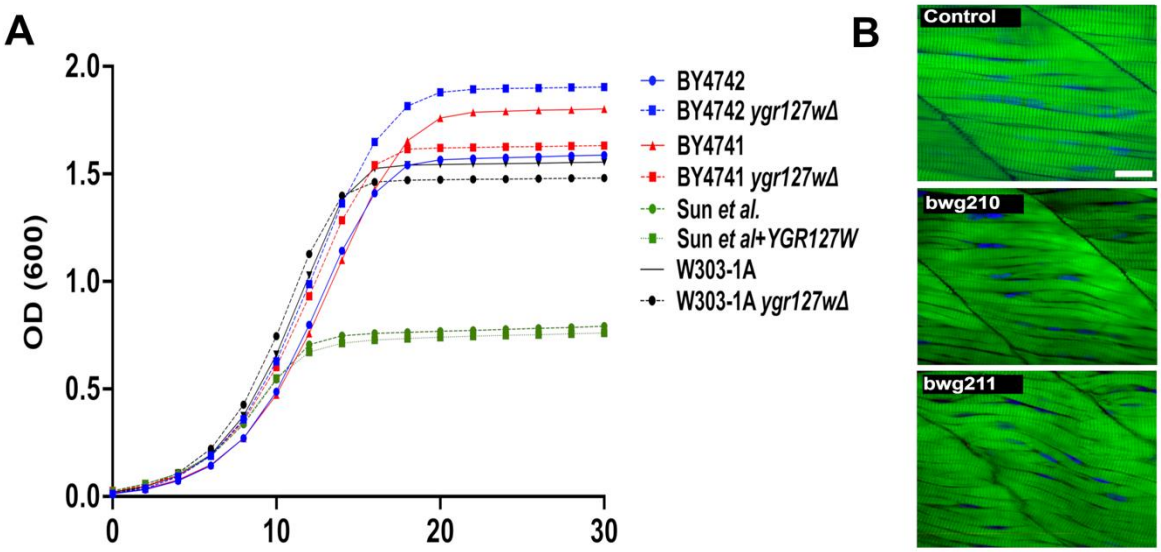

Figure 4: Growth and muscle fiber integrity in yeast and zebrafish models of TANGO2 deficiency fail to replicate previously reported phenotypes.

A) Yeast growth curves. Different strains were grown in SC medium or SC medium lacking histidine at 25º C. **B)** Whole mount phalloidin staining of control and two strains of *tango2*$^{-/-}$ zebrafish (*bwg*^{210} and *bwg*^{211}). Myofibers in mutants lack the parallel organization observed in controls but do not demonstrate significant myofiber breakdown or damage. Representative images; N=8-10 in each group. Scale bar=5 μm.